JOURNAL OF APPLIED ELECTROCHEMISTRY 19 (1989) 401–409

Electrocoating of iron and other metals with polypyrrole

M. SCHIRMEISEN, F. BECK

University of Duisburg, FB 6 – Elektrochemie, Lotharstr. 1, D-4100 Duisburg 1, FRG

Received 19 April 1988; revised 27 October 1988

Galvanostatic electrodeposition of polypyrrole from more than 20 nonaqueous and aqueous electrolytes containing anions such as BF_4^-, ClO_4^-, HSO_4^-, SO_4^{2-}, Tos^-, HCO_3^-, $H_2PO_4^-$, HPO_4^{2-}, $H_2BO_3^-$ and NO_3^- at the substrates Pt, Au, Cu, Ti, stainless steel/V2A and Fe was investigated. The passivating substrates Pt, Au, Ti and V2A could be electrocoated under a broad variety of conditions. Cu dissolved anodically. The same was true for Fe with only one important exception, namely aqueous nitrate. Smooth, well-adhering polypyrrole layers were obtained on iron at NO_3^- concentrations of 0.01–1 M and at current densities of 0.5–10 mA cm^{-2}. The degree of insertion for nitrate ions was about $y = 0.25$, confirmed by elemental analysis. Current efficiencies with regard to this y were about 90%. The layers were stable in air for a long time.

1. Introduction

Galvanization of metals for corrosion protection and decoration has been known for a long time. Thin layers of nickel, chromium, zinc, silver, etc. are cathodically electrodeposited usually at constant current densities. In the last 10 years conducting polymers have been widely investigated. In many cases, these new materials are synthesized at an inert anode such as platinum, gold or glassy carbon, to yield coherent layers with an electronic conductivity in the range of 1–1000 S cm^{-1}. This is high enough to rule out any excessive ohmic drop at the layer, even in the case of extended thickness growth. Most of the previous work deals with the electrosynthesis of the new materials and with their investigation as a metal/polymer sandwich or, after detachment of thick layers from the substrate, as free standing polymer films. Surprisingly, the electrocoated metal itself has not yet been studied in detail. Nevertheless, it seems to be an interesting question to compare these electrocoated metals with galvanized metals. In Table 1, some important properties of typical coatings are compiled.

Specific conductivity and tensile strength differ by four orders of magnitude. The main difference between the two types of electrocoating is the direction of current flow. However, in both cases, cation and anion transfer rather than electron transfer is the potential determining process. The growth of a solid phase upon electrodeposition onto a substrate is a complicated multistep process. From a polymer point of view, the film-forming electropolymerization of aromates and heteroaromates must be compared with electropolymerization of vinylmonomers and with electrocoagulation of ionomers [3, 4]. It is only the last mentioned process which has found a broad application in the electrodeposition of paint.

Polypyrrole is the most flexible candidate amongst the conducting polymers, for its electrodeposition can proceed under a wide variety of conditions, both from aqueous [3–8] and from nonaqueous [9–11] electrolytes. The standard nonaqueous electrolyte, proposed by Diaz *et al.*, is acetonitrile with NR_4ClO_4 or NR_4BF_4 (R = Et or Bu). However, as already stated by these workers and confirmed recently by Pletcher *et al.* [12], the addition of about 1% water greatly improves the quality of the electrodeposited polypyrrole layer. Most of the work on polypyrrole in the last few years has been devoted to these types of nonaqueous electrolytes. As already mentioned, inert substrates such as Pt, Au or GC have been preferred to practical substrates such as Fe, Al, Cu, Ti, Ni stainless steel, etc. Aqueous electrolytes have not been systematically employed. Typical parameters such as temperature, stirring rate, current density or presence of oxygen have not been investigated in detail. It is the aim of this paper to provide new information in this area.

2. Experimental details

Pyrrole (Janssen) was freshly distilled under N_2. Its standard concentration was 0.1 M. As solvents, acetonitrile (Merck zur Synthese, 0.05% H_2O after drying over molecular sieve 3 Å), methanol (distilled) and water (double distilled) were employed. The salts of p.a. quality were used as such; tetrabutylammoniumtetrafluoborate (TBAT) was from Fluka (purum) and contained about 1 mM Br^-, which acts as a catalyst [13] improving the rate of electrodeposition appreciably.

The electrodes used for the determination of the electrochemical equivalent, m_e, were sheets of dimension 35 × 60 mm ($A = 42$ cm^2), with a current lead at the small side. The following modes of preparation

0021-891X/89 $03.00 + .12

Table 1. Comparison of copper and polypyrrole electrocoatings

	Copper	Polypyrrole
(1) Electrochemical equivalent m_e (mg C^{-1})	0.33	0.40
(2) Specific conductivity κ (S cm^{-1})	10^6	10^2
(3) Typical current densities for electrodeposition (e.d.) j (mA cm^{-2})	−(10–20)	+(0.2–2)
(4) Typical potentials for e.d. U_K (V vs SCE)	0	0.9 in MeCN 0.6 in H_2O
(5) Density ϱ (g cm^{-3})	8.9	1.5
(6) Tensile strength ε (N mm^{-2})	10^5	50 [1, 2][1]

[1] This large value only holds for aromatic sulphonates as anions. For more usual anions such as BF_4^-, ε is smaller by one order of magnitude.

were employed: platinum (0.1 mm): 10 min chromic acid (100° C) with subsequent 10 min boiling in 20% HCl. Other metals (1 mm): polishing with wet Al_2O_3 powder. The other metals were: iron (C-steel, St 37), copper (99.9%), stainless steel (V2A, 18/8 Cr/Ni) and titanium (Contimet 31, Thyssen Edelstahlwerke). Titanium was subsequently etched for 1 h in 20% HCl at 95° C. Small electrodes (0.5–2 cm^2) were used for the voltammetric measurements. Here, Au and Ni were used additionally. Counter electrodes made of stainless steel, were arranged on both sides of the working electrode. The reference electrode was a saturated sodium chloride calomel electrode (SSCE), which has a potential of +236 mV vs SHE. The potentials, measured vs this reference, are named U_{SSCE}.

Electrodeposition of polypyrrole at the various substrates was performed under galvanostatic conditions (j = 0.5–2 mA cm^{-2}), mostly in slowly stirred solutions at 20° C under argon. Voltammetric measurements were performed with a potentiostat (HEKA PG 284) with an integrated voltage scan generator and coulometer, together with an XY recorder (Hewlett Packard 7046 b).

The electrocoated electrodes were thoroughly extracted in boiling methanol, as described previously [14]. After drying at room temperature the mass of the electrodeposit was determined with a semimicrobalance (Sartorius R 160 P) with an accuracy limit of 0.01 mg.

3. Results

3.1. *Definition of a nominal layer thickness, d_n*

Polypyrrole is formed by anodic α,α-coupling of pyrrole rings. At the potential of the electropolymerization, every segment of the conjugated backbone, containing three or four monomer units, is further oxidized to yield the polymeric radial cation. The overall process can be written as

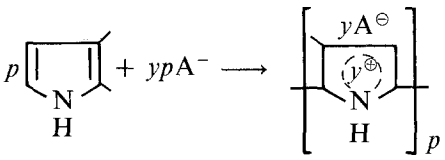

$$+ 2(p - 1)H^+ + [p(2 - y) - 2]e^- \quad (1)$$

where p is the degree of polymerization, and y a stoichiometric factor. The four C–H bonds in the monomer and the remaining two C–H bonds in the polymer are marked. A^- is the anion, which is inserted for charge compensation. From this model, the theoretical electrochemical equivalent $m_{e,th}$ for polypyrrole can be easily derived to be

$$m_{e,th} = \frac{M}{zF} = \frac{M_M + yM_A}{(2 + y)F} \quad (2)$$

where M_M is the molecular weight of the monomer unit in the polymer ($M_M = M_{py} - 2 = 65$) and M_A is the molecular weight of the anion. y is the above mentioned degree of insertion. Obviously, Equation 2 is only valid for high degrees of polymerization p. The exact relationship for limited values of p was derived earlier [14]. A nominal thickness, d_n, of the polymer layer follows from Equation 2 using Faraday's law:

$$d_n = \frac{Q_A}{\varrho} \frac{M_M + yM_A}{(2 + y)F} = \frac{Q_A m_e}{\varrho} \quad (3)$$

where ϱ is the density of polypyrrole, which was found to be 1.50 for BF_4^--doped polypyrrole [10, 15]. We confirm this figure, but a highly porous structure with 50–80% free pore volume was measured at the same time [16]. This indicates that the high inner surface of the polymer is perfectly wetted in the course of the floating method which has been employed for the den-

Table 2. Examples for m_e and d_n for polypyrrole, doped with various anions

	M_A	$m_{e,th}$ (mg C^{-1})		d_n (μm) for Q_A = 0.4 C cm^{-2}	
		y = 0.25	y = 0.33	y = 0.25	y = 0.33
BF_4^-	87	0.400	0.417	1.07	1.11
ClO_4^-	99.5	0.413	0.435	1.10	1.16
$CH_3(C_6H_4)SO_3^-$	171	0.496	0.540	1.32	1.44

Table 3. Current efficiencies (%) for the galvanostatic deposition of polypyrrole from nonaqueous electrolytes. Slow stirring, $d_n = 1.5\,\mu m$

Electrolyte 0.1 M pyrrole +	Anode	Current density ($mA\,cm^{-2}$)		
		0.2	2	20
I 0.1 M NBu_4BF_4	Pt	95	105	50
0.001 M Br^- in MeCN	V2A	67	107	60
	Ti	108	123	64
	Fe	(−45)	(−97)	(−96)
	Cu	(−80)	(−98)	(−100)
II 0.1 M $NaClO_4 \cdot H_2O$ in MeCN	Pt	133	128	71
	V2A	128	123	51
	Ti	120	124	13
	Fe	(−107)	(−103)	(−121)
III 0.1 M NEt_4^+ $(CH_3\text{-}C_6H_4\text{-}SO_3)^-$ (*p*-toluenesulphonate) in MeCN	Pt	82	90	91
	V2A	92	116	85
	Ti	85	88	92
	Fe	(−29)	(−98)	(−12)
IV 0.013 M $NaNO_3$ in MeCN	Pt	94	82	–
	V2A	90	61	–
	Ti	81	39	–
	Fe	(−90)	(−135)	–
V 0.1 M $NaClO_4 \cdot H_2O$ in methanol	Pt	140	135	117
	V2A	116	105	14
	Ti	31[1]	46[1]	24[1]
	Fe	(−82)	(−82)	(−100)

[1] No visible black polymer layer

sity measurements. Q_A is the area specific overall charge for electropolymerization. Table 2 represents some examples for $m_{e,th}$ and d_n for polypyrrole with various inserted anions.

For $A^- = BF_4^-$, experimental values for m_e (0.36 . . . 0.45 mg C^{-1} [10]) scatter around the theoretical figure in Table 2. Lundström *et al.* [17] report a thickness of $d = 1.6\,\mu m$ for $Q_A = 1\,C\,cm^{-2}$, while it should be 2.68 μm, starting from the d_n in Table 2. These few examples indicate that m_e or d_n is not exactly defined.

In the following, a current efficiency, c.e. = γ will be derived from the measured electrochemical equivalent

$$m_e = m/Q \tag{4}$$

where m is the mass of the electrodeposited polypyrrole and Q is the charge applied. The current efficiency γ is then given as

$$\gamma = m_e/m_{e,th} \tag{5}$$

The charge applied will be indirectly defined in terms of nominal thickness d_n according to Equation 3. For y, a value of 0.25 has been assumed.

3.2. *Electrodeposition in nonaqueous electrolytes*

Table 3 compiles the current efficiencies for the electrodeposition of polypyrrole in four electrolytes with acetonitrile and one with methanol on to 4–5 different substrates. The layer thickness was $d_n = 1.5\,\mu m$. The electrolytes tested in this connection did not lead to a deposit on iron and copper. These metals were anodically dissolved and the negative current efficiencies in parentheses refer to the mass loss in the anodic processes

$$Fe \longrightarrow Fe^{2+} + 2e^- \tag{6}$$

and

$$Cu \longrightarrow Cu^+ + e^- \tag{7}$$

respectively. Even the nitrate electrolyte, which allowed the electrodeposition at iron in the aqueous solution, was not successful in acetonitrile. In this case, the saturated electrolyte contained 0.013 M $NaNO_3$.

Only the three other metals lead to a coherent, well-adhering, black polypyrrole layer, at least for the two lower current densities. For platinum and electrolyte I, the current efficiencies are close to 100% for the lower current densities. This also holds for a broad variety of d_n from 0.01 μm up to 100 μm [14]. C.e. appreciably decreases at the highest current density for nearly all electrolytes and all anode materials. This is due to the overoxidation of the polypyrrole [18], leading to soluble products of oxidation, which is also indicated by a rapid colouring (brown to black) of the electrolyte. Under these conditions, the electrodeposited layer was uneven and had only a poor quality. In some cases, a virtual c.e. well above 100% is observed, indicating the coinsertion of solvent and/or the formation of an additional oxide interlayer. In the case of titanium, no black polymer could be detected for the methanolic electrolyte. This may be connected with the anodic dissolution of titanium in pure methanol, which can be inhibited upon the addition of 10 wt% water [19]. However, electrodeposition of polypyrrole onto titanium from the acetonitrile electrolytes led to good deposits with excellent adherence. Stainless steel V2A behaved, in every respect, very similarly to platinum. Again, the only exception was the meth-

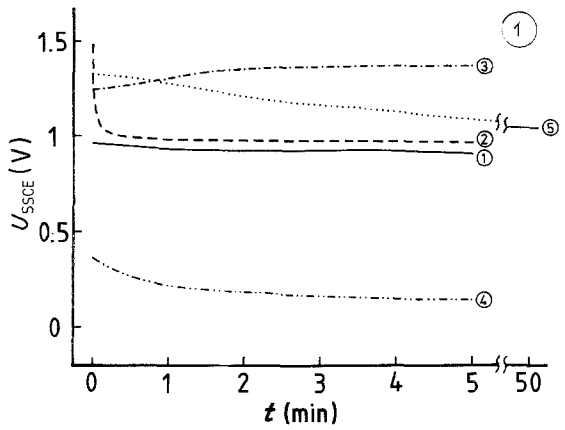

Fig. 1. Potential–time curves for the galvanostatic electrodeposition of polypyrrole (d_n = 1.5 μm) from electrolytes in acetonitrile at various substrates: (1) 0.1 M NBu_4BF_4, at Pt; (2) 0.1 M NBu_4BF_4, at V2A; (3) 0.1 M NBu_4BF_4, at Ti; (4) 0.1 M NBu_4BF_4, at Fe; (5) 0.013 M $NaNO_3$, at Fe. The current density for (1)–(4) was 2 mA cm^{-2}, for (5) 0.2 mA cm^{-2}.

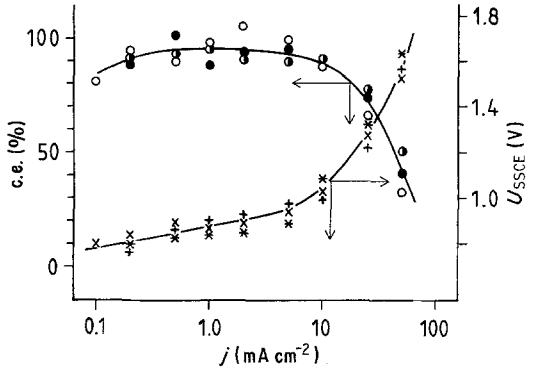

Fig. 2. Current efficiencies (c.e.) and working potential U_{SSCE} in dependence on current density for three d_n for the galvanostatic electrodeposition of polypyrrole from electrolyte I (0.1 M NBu_4BF_4 in MeCN) at platinum, slow stirring, 20° C. c.e. for d_n = 0.8 μm (○), 2.7 μm (◑) and 8.1 μm (●). U_{SSCE}/V for d_n = 0.8 μm (x), 2.7 μm (+) and 8.1 μm (*).

anolic electrolyte, where the c.e. broke down at the highest current density. Nevertheless, an even, well-adhering polypyrrole layer, was observed under this condition.

Most of the polypyrrole layers had a matt appearance due to an appreciable surface roughness even at this small thickness. However, the tosylate electrolyte III was an exception and smooth, bright deposits were obtained.

The potential–time curves for some characteristic examples are shown in Fig. 1. While the potential in the case of the formation of a coherent polypyrrole film on Pt, V2A and even on Ti is fairly constant at about 0.9 V vs SSCE, it breaks down for iron as a substrate to the active potential in NBu_4BF_4 as well as in $NaNO_3$. The potential of electropolymerization cannot be reached with this anode material under the present conditions.

The current density, j, was varied between 0.1 and 50 mA cm^{-2} for electrolyte I at platinum. For a c.d. higher than 5 mA cm^{-2}, a decreasing c.e. and an increasing potential indicates the crossing of the limit to overoxidation, cf. Fig. 2. However, this is only possible due to the presence of 1 mM Br^- as catalyst

Table 4. Current efficiencies (%) for the galvanostatic deposition of polypyrrole from aqueous electrolytes. Slow stirring, j = 2 mA cm^{-2}, 20° C

Electrolyte 0.1 M pyrrole +		Anode	Nominal thickness d_n (μm)		
			1	3	10
VI	0.1 M $NaBF_4$	Pt	87	89	87/86[1]
		V2A	84	87	85
		Fe	(−209)	(−179)	(−95)
VII	0.1 M $NaClO_4$	Pt	88	90	90
		V2A	83	92	90
		Fe	[2]	(−116)	(−96)
VIII	0.1 M $NaHSO_4$	Pt	82	79	70/71[1]
		V2A	79	74	6
		Fe	(−209)	(−159)	(−103)
IX	0.1 M Na_2SO_4	Pt		81	
		Fe		(−96)	
X	0.1 M KNO_3	Pt	92	90	89/86[1]
		V2A	86	86	88
		Fe	88	88	88
		Ti	–	90/79[3]	–
XI	0.1 M $NaHCO_3$ (pH 8)	Pt		7	
		Fe		[2]	
XII	0.1 M $Na_2B_4O_7$ + 0.1 M H_3BO_3 (pH 9)	Pt		5	
		Fe		[2]	
XIII	0.1 M NH_2SO_3H (amidosulphonic acid)	Pt	87	87	
		V2A	82	78	
		Fe	(−140)		
XIV	0.1 M NH_2SO_3Na (pH 3)	Pt	24	10	
		V2A	43	12	
		Fe	(−150)		

[1] Two independent runs to check reproducibility.
[2] Positive mass balance, but no polypyrrole film.
[3] Two different modes of pretreatment: mechanically/1 h etching 20% HCl at 90° C.

[13]. In its absence, this limit would be lower by one order of magnitude. Diaz recommends a current density as low as 0.1–1 mA cm^{-2} [9–11].

Variation of temperature in the range 0–70° C for the standard electrolyte I and a galvanostatic electropolymerization at platinum with 2 mA cm^{-2} had no marked effect on the c.e. It was fairly constant at about 90% for d_n = 1 μm and 10 μm up to 50° C. Only at 60 and 70° C was some decrease observed, down to about 80 and 70%. The potential tended to become more negative.

Addition of water to enhance its concentration from the original level of about 0.1% to 0.4, 1.2 and 3.5% (standard electrolyte I, Pt, 0.5 mA cm^{-2}, d_n = 0.8–2.7 and 8 μm) did not influence c.e. and the quality of the polypyrrole layer.

3.3. *Electrodeposition in aqueous electrolytes*

Aqueous electrolytes, which must be preferred from a practical point of view, have been mainly investigated under neutral or acid pH conditions. Due to the generation of protons according to Equation 1, the diffusion layer becomes acid, in the normal case, and nucleophilic attack of OH^- ions is prevented [20].

Table 4 represents the results for some aqueous electrolytes at three levels of d_n. Electrodeposition was performed at platinum, stainless steel and iron. Current efficiencies are somewhat lower for Pt and V2A in comparison with the nonaqueous electrolytes. Potentials are more negative. Na_2SO_4 gave similar results to $NaHSO_4$, in spite of the bivalent anion. Bicarbonate (XI) and borate (XII) led to very poor deposits, presumably due to the elevated pH in solution, which promotes overoxidation.

As previously, iron could not be electrocoated with polypyrrole. Iron anodically dissolved according to Equation 6, indicated by the negative c.e. or insoluble corrosion product accumulation at the iron surface. In this case, a positive mass balance was found, but no black polypyrrole layer. These examples are labeled with an asterisk. However, there is one remarkable exception, namely the nitrate electrolyte No. X. Only with this electrolyte could normal polypyrrole layers

Table 5. Current efficiencies (%) for the galvanostatic deposition of polypyrrole from aqueous electrolytes containing phosphate ions. Slow stirring, j = 2 mA cm^{-2}, 20° C

Electrolyte 0.1 M pyrrole +		Anode	Current efficiency for d_n = 3 μm	pH
XV	0.1 M NaH_2PO_4	Pt	ca. 40	4.5
		V2A	ca. 50	
		Fe	(−92)	
XVI	0.1 M NaH_2PO_4	Pt	81	4.5
	+ 0.1 M $NaBF_4$	V2A	79	
		Fe	(−136)	
XVII	0.1 M Na_2HPO_4	Pt	ca. 5	9.5
		Fe	[1]	
XVIII	0.1 M Na_2HPO_4	Pt	37	9.5
	+ 0.1 M $NaBF_4$	Fe	[1]	
XIX	0.1 M NaH_2PO_4	Pt	70	4.5
	0.01 M KNO_3	Fe	(−105)	
XX	0.1 M Na_2HPO_4	Pt	16	9.5
	0.01 M KNO_3	Fe	[1]	
XXI	0.1 M NaH_2PO_4	Pt	6	≈6
	0.01 M $Na_2B_4O_7$	Fe	±0	

[1] Positive mass balance, but no polypyrrole film.

be electrodeposited onto iron sheets. Besides the standard iron sheets, we succeeded in electrocoating panels of steel (St 37), of dimension 10.5 × 20 cm from 0.1 M KNO_3. The current density was 2 mA cm^{-2}. The solutions were not deaereted in this case. The electrolyte circulated parallel to the panels with a flow rate of 1 cm s^{-1}. Even, well-adhering coatings of polypyrrole on iron were obtained with a nominal thickness of d_n = 0.3–0.7 μm after rinsing with methanol and drying in air. As a single electrolyte, KNO_3 was suitable over a wide range of concentrations. Figure 3 demonstrates that current efficiencies for anodic polypyrrole formation on iron remain high at KNO_3 concentrations from 10 mM to 1 M. They show a continuous increase with increasing concentration at both Fe and Pt. In 0.1 M KNO_3, current efficiencies for polypyrrole were 85–90% at current densities of 0.2 or 2 mA cm^{-2}. No marked difference to other substrates such as Pt or V2A were observed. For iron at 20 mA cm^{-2}, the c.e. dropped to 40–50%, cf. Fig. 2 (for platinum). At 2 mA cm^{-2}, the c.e. for 40° C was the same as that for 20° C.

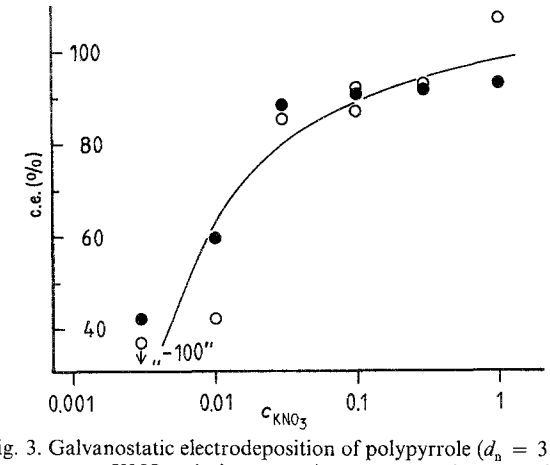

Fig. 3. Galvanostatic electrodeposition of polypyrrole (d_n = 3 μm) from aqueous KNO_3 solutions at various concentrations: ○ at iron; ● at platinum. j = 2 mA cm^{-2}, 20° C, slow stirring.

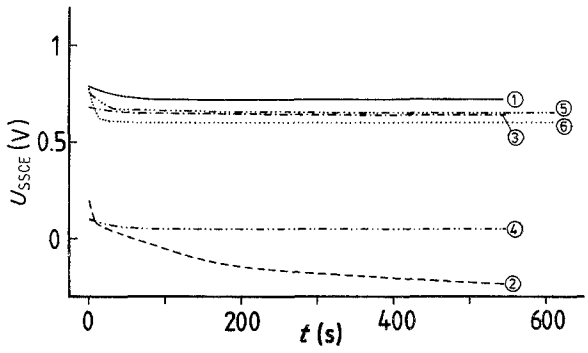

Fig. 4. Potential–time curves for the galvanostatic electrodeposition of polypyrrole (d_n = 3 μm) from aqueous electrolytes at various substrates: (1) 0.1 M $NaClO_4$, at Pt; (2) 0.1 M $NaClO_4$, at Fe; (3) 0.1 M $NaHSO_4$, at Pt; (4) 0.1 M $NaHSO_4$, at Fe; (5) 0.1 M KNO_3, at Pt; (6) 0.1 M KNO_3, at Fe. The current density was 2 mA cm^{-2}.

However, addition of an inert electrolyte to improve conductivity was not possible, as is proved by some examples in Table 5. Amidosulphonic acid, carrying another N-containing inorganic anion, was not successful, neither as the free acid (No. XIII) nor as the salt (No. XIV). Even platinum behaved as usual only in the presence of the free acid. As a salt, the low c.e. may be due to the nucleophilic attack of the amino function.

Figure 4 shows some representative potential time curves. The cases with a positive, constant potential are for the electrodeposition of a coherent polypyrrole layer. In the two systems (2) and (4) with iron substrate, practically no deposit was found due to the negative electrode potentials. Again, only in the presence of NO_3^- was an electrodeposit observed at iron at relatively positive potentials (curve 6).

We also evaluated phosphate-containing electrolytes to find a second example of a bath from which electrocoating of iron substrates with polypyrrole would be feasible. In spite of the fact that phosphate ions promote the passivations of iron, all these attempts failed. Table 5 gives some details for these runs. It can be recognized that platinum is a suitable substrate as long as the pH does not shift to the alkaline region. The poor c.e. for secondary phosphates (systems XVII, XVIII and XX) is attributed to the same overoxidation effect as for the bicarbonate and borate electrolytes XI and XII in Table 4. The iron substrates dissolved smoothly in the acid electrolytes, but they were covered with a well-adhering inorganic layer in the case of the alkaline systems. Pitting corrosion was occasionally observed in the alkaline region. Even an anodic prepassivation of iron in HNO_3 or NaOH did not prevent the subsequent anodic dissolution of the metal in 0.1 M pyrrole/0.1 M $NaBF_4$.

3.4. *Voltammetric results*

Electrodeposition of polypyrrole from the nonaqueous electrolyte at platinum proceeds at relatively positive potentials according to a combined electrochemically forced polymerization/precipitation mechanism. As Fig. 5 shows, a kinetically limited prewave is found, which depends on the water concentration after a reaction order of 0.5–0.9, depending on the anion [21].

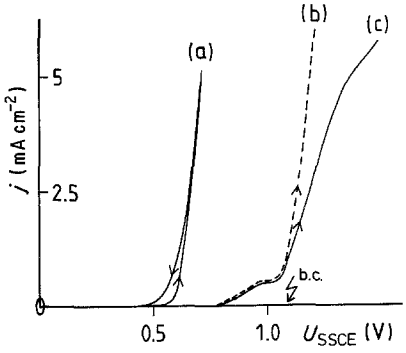

Fig. 5. Voltammetric curves for the potentiodynamic electrodeposition of polypyrrole at platinum, $v_s = 2\,mV\,s^{-1}$, 0.1 M pyrrole: (a) +0.1 M $NaBF_4$ or 0.1 M KNO_3 (identical curves) in water; (b) +0.1 M $LiClO_4$ in MeCN, 0.01 M H_2O; (c) +0.1 M NBu_4BF_4 in MeCN, 0.01 M H_2O. b.c. = basic curve.

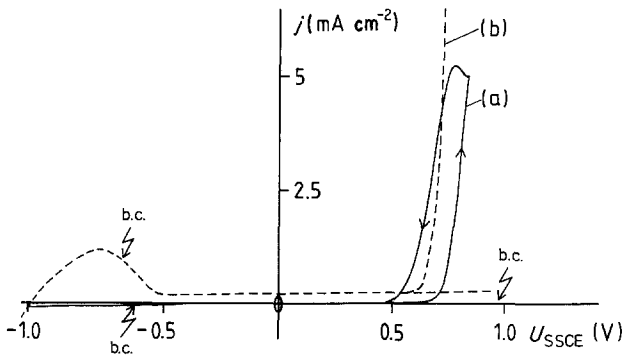

Fig. 6. Voltammetric curves for the potentiodynamic electrodeposition of polypyrrole at titanium, mechanically pretreated, $v_s = 2\,mV\,s^{-1}$, 0.1 M pyrrole: (a) +0.1 M KNO_3 in H_2O; (b) +0.1 M $NaBF_4$ in H_2O. b.c. = basic curve.

The electrodeposition curve in aqueous electrolytes at platinum leads to a current voltage curve shifted in the negative direction. Obviously, no prewave is found in this case. The curves do not depend significantly on the anion; they are essentially the same in tetrafluoborate and in nitrate solutions. This does not hold for a gold anode, where in the case of nitrate in aqueous electrolytes, a much more pronounced hysteresis is observed. Stainless steel behaves similarly to platinum; the transpassive dissolution of chromium in $NaBF_4$ starts at potentials which are about 300 mV more positive. Titanium is electrocoated from both aqueous electrolytes at potentials around those at platinum. The only difference lies in the basic curve, as shown in Fig. 6. While in the case of the nitrate electrolyte the metal is in the passive state over a wide potential region, the $NaBF_4$ electrolyte exhibits an activated dissolution at $U_K = -1\,V$. This may be due to the presence of fluoride ions after partial hydrolysis of BF_4^-. Finally, the electrochemical behaviour of the iron anode is shown in Fig. 7. The electrode clearly remains in the active state for $NaBF_4$ up to high current densities while, in the case of KNO_3, a medium activated region is observed which enters into a passive domain. Finally, a complicated deposition curve is seen with a large, reproducible hysteresis. The dissolution peak is diminished in the presence of pyrrole in spite of the complexation properties of pyrrole for iron ions.

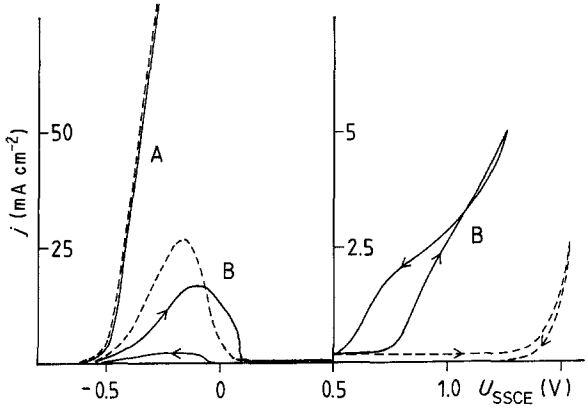

Fig. 7. Voltammetric curves for the potentiodynamic electrodeposition of polypyrrole at iron, $v_s = 2\,mV\,s^{-1}$, 0.1 M pyrrole: (A) +0.1 M $NaBF_4$ in H_2O; (B) +0.1 M KNO_3 in H_2O. The corresponding basic curves are drawn as ----.

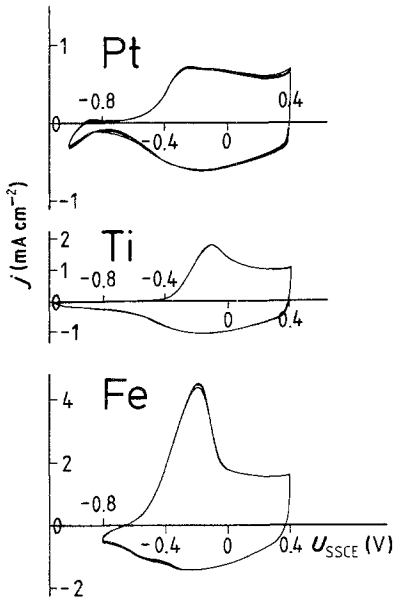

Fig. 8. Cyclic voltammetric curves for the polypyrrole layers according to Figs 5–7, $v_s = 20\,mV\,s^{-1}$, 0.1 M aqueous KNO_3. The following charges (in mC) for electrodeposition Q_0, charge Q_+ and discharge Q_-, both for the second to fifth cycle, were measured: Pt, $A = 0.5\,cm^2$, $Q_0 = 150$, $Q_+ = 13.8$, $Q_- = 13.2$; Ti, $A = 1\,cm^2$, $Q_0 = 554$, $Q_+ = 44.5$, $Q_- = 44.5$; Fe, $A = 1\,cm^2$, $Q_0 = 855$, $Q_+ = 104$, $Q_- = 59$.

As shown in Equation 1, the polypyrrole is deposited in a doped state. On potentiodynamic polarization in the negative direction, the primary discharge occurs in the region negative to 0.4 V [14]. The polypyrrole layer can be cycled in the region of +0.4 to −0.8 V or −1.5 V. No dramatic differences in the cyclovoltammetric features can be seen. Figure 8 gives three examples corresponding to the coatings described in Figs 5–7. Surprisingly, the current efficiency for cycling the layer on Ti is quantitative, but not so for the layer on platinum. For iron, a low Q_-/Q_+ ratio is found (0.57) and the anodic peak is much more pronounced. Even in this case, the cycles are absolutely reproducible. The degrees of insertion, y, calculated with $y = 2Q_-/(Q_0 - Q_-)$, are 0.19, 0.17 and 0.15, respectively.

3.5. *Nonelectrochemical results*

The surface roughness of the polypyrrole layers increases with increasing current density. SEM pictures exhibit 'cauliflower structures', especially for thick layers [11, 14, 32]. The other side of the film, adhering to the smooth substrate, is relatively featureless. Adherence of the polymer layers increases with decreasing thickness and with increasing water concentration in acetonitrile and roughness of the substrate. Quantitative determinations are under way.

Elemental analysis of the polypyrrole layers electrodeposited from acetonitrile electrolyte reveals an excess of hydrogen and a minor deficit of nitrogen [9, 10, 13, 23, 24]. The reasons for this were discussed [13] in terms of low degrees of polymerization and/or coinsertion of solvent. Results for aqueous sulfuric acids are similar [6]. Table 6 collects some of our own findings in aqueous electrolytes.

Table 6. Elemental analysis of polypyrrole on platinum in terms of $C_4H_wN_x \cdot yA^-$. The polymer was electrodeposited from aqueous electrolytes

0.1 M electrolyte	w	x	y	
			From 100 −(C + H + N)%	From master element
$NaBF_4$	3.4	0.94	0.36	0.02 (F)
$NaClO_4$	3.1	1.0	1.1	0.20 (Cl)
KNO_3 at Pt	3.1	1.20	0.50	0.20 (N)[1]
KNO_3 at V2A	2.9	1.16	0.40	0.21 (N)[1]
KNO_3 at Fe	3.0	1.18	0.52	0.23 (N)[1]
NaH_2PO_4	2.9	0.96	0.36	0.12 (P)
$NaHSO_4$	2.8	0.96	0.28	0.12 (S)

[1] Assuming x for monomer unit to be 0.95

The hydrogen stoichiometry is now closer to theory ($w = 3.0$). Surprisingly, even for the two last mentioned anions with hydrogen, the value for w lies below the theoretical value of 3.6 or 3.3. The degree of insertion y was either derived from the difference of the C/H/N composition up to 100% or from the direct determination of the characteristic element (in parentheses) in the given anion. The former results are much too high, indicating further components to those in Equation 1 to be present in the doped polypyrrole. On the other hand, the direct fluorine determinations in polypyrrole with inserted BF_4^- led to a y which is much too low, as was previously stated by Diaz [9, 10, 15].

Curiously enough, attempts at a direct spectroscopic determination of the anions in doped polypyrrole with the help of IRRAS (IR reflection absorption spectroscopy at thin layers [25]) totally failed. As is shown in Fig. 9, the spectra coincide in spite of the fact that various anions are inserted, having characteristic absorption bands in the free states or even as a salt in this region. This phenomenon may be explained in terms of a total steric hindrance of the IR oscillations in the case of an anion inserted in the polymer structure.

4. Discussion

Anodic electrodeposition of polypyrrole layers in the

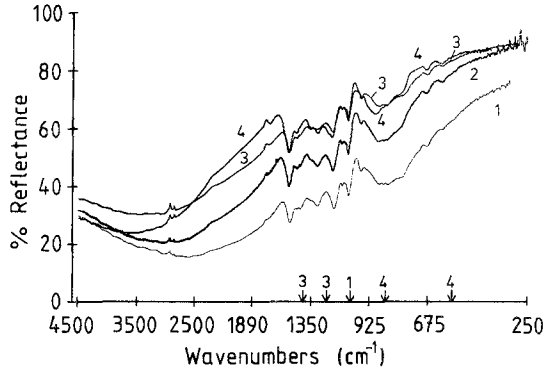

Fig. 9. IRRAS spectra for polypyrrole layers ($d_n = 0.3\,\mu m$) electrodeposited from acetonitrile solutions containing the following electrolytes (0.1 M): (1) NBu_4BF_4; (2) NEt_4-tosylate; (3) NEt_4EtSO_4; (4) $LiPF_6$. The arrows indicate the wave numbers, where strong adsorption of the anions would be expected.

doped state is possible over a wide variety of conditions. At low current densities, the experimentally determined electrochemical equivalents led to a current efficiency of 80–100% under the assumption that oxidative coupling of the pyrrole rings proceeds in the α,α' position and that every fourth monomer unit in the polymer is further oxidized to the radical cation after which an anion is inserted to compensate the positive charge. According to this stoichiometry, a nominal thickness, d_n, was defined with the experimental density of $1.5\,g\,cm^{-3}$ for the doped polymer, cf. Section 3.1. As pointed out above, d_n is only a relative figure for the classification of the layers due to the fact that a free pore volume of 50–80% had been experimentally found [16].

Our results show that electrodeposition proceeds smoothly in many aqueous electrolytes, if passive metals such as Pt, Au, V2A or Ti are employed as a substrate. More than 15 aqueous electrolytes were successfully tested. Among these, anions such as $H_2PO_4^-$ or $NH_2SO_3^-$ were used for the first time. However, the situation totally changes if nonpassive metals such as copper or iron are used. The metal actively dissolves (at least at a pH below 7) and no electrocoating is possible. At higher pH, about 10, these metals also passivate, but inorganic layers are built rather than a polymer film, or c.e. for the overoxidized polymer is poor and soluble anodic products are generated from the monomer. The only exception from this rule was found to be the nitrate ion. An excellent electrocoating from an aqueous bath of KNO_3 and pyrrole can be achieved on iron. This holds for a wide range of electrolyte concentrations. Dissolved oxygen does not interfere. Well-adhering, smooth layers are obtained even on larger panels of this metal. Potential–time curves for the electrodeposition at a constant current density (Fig. 4) and voltammetric curves (Fig. 7) reveal that the potential for electrodeposition lies relatively positive, if one compares it with other metals such as Pt. In spite of a large potentiodynamic dissolution peak in the active region, cf. Fig. 7, the galvanostatic electrodeposition is feasible at moderate current densities. From the N value of elemental analysis, a degree of insertion of 0.2–0.23 is derived (Table 6), which is within the range found for other anions. The exceptional behaviour of nitrate ions may be correlated with the tendency of the nitrate ion to yield radicals at the anode, thus initiating a radical oxidation of the organic compound, cf. [26]. However, this is normally assumed for nonaqueous systems, and a radical mechanism would contradict the ionic mechanism usually assumed for the electropolymerization of pyrrole.

Electrodeposition of polypyrrole with a systematic variation of the metal substrate has been investigated by Lundström *et al.* [17]. Evaporated metal films of thickness 300 nm were employed. The electrolyte was 0.1 M NEt_4BF_4 in acetonitrile. In accordance with our results, iron could not be electrocoated. The other metals, which anodically dissolved, were Al, In and Ag. Recently, electrocoating of Fe and Al with polypyrrole was accomplished from pyrrole solutions in propylene carbonate in the presence of NEt_4–tosylate [37]. Two reports for the electrodeposition of polypyrrole in the presence of nitrate on polished platinum (or glassy carbon) from Pletcher *et al.* [7] and on gold from Warren and Anderson [8] are available. The solvent was water in both cases. In the latter work, uneven irreproducible deposits were found. This may be a special feature of the gold substrate, where we also found irregular voltammetric curves, cf. Fig. 10. Electrodeposition onto nonmetallic substrates has been occasionally reported, namely for tin oxide [15], *n*-silicon [27, 28], CdS [29], GaAs [30] and WSe_2 [31]. Electrodeposition of metals onto polypyrrole films was investigated by Chandler and Pletcher [32].

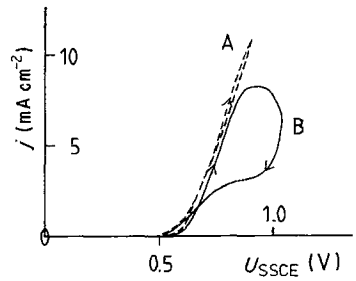

Fig. 10. Voltammetric curves for the potentiodynamic electrodeposition of polypyrrole at gold, $v_s = 2\,mV\,s^{-1}$, 0.1 M pyrrole: (A) – – – 0.1 M $NaBF_4$ in H_2O; (B) —— 0.1 M KNO_3 in H_2O.

The polypyrrole layer is primarily electrodeposited in the doped state. Figure 8 shows three examples of the so-called switching curves. The presence of anions in the polymer film is an inherent disadvantage, and it may stimulate corrosion of the substrate and contaminate the adjacent phase. The layer itself may corrode under atmospheric conditions and a release of the anions may be the consequence. Corrosion of polypyrrole layers was studied with the aid of conductivity measurements [33, 34] and by periodic determination of the residual charge [35]. Cathodic undoping leads to the removal of the anion, but the undoped polymer is rapidly autoxidized in the air. Another strategy is the anodic release of the anions. Upon slow anodic polarization, the anions are also expelled and the reactive cationic centers are saturated with present nucleophiles [36]. Overoxidized polypyrrole [18] may have a better adherence due to the enhanced polarity of the backbone. These and other improvements may finally lead to modified polypyrrole layers which are able to protect the substrate effectively from corrosion. They can also be used as interlayers, e.g. for electrodeposition of paint.

Acknowledgements

Financial support of this work by AIF (Arbeitsgemeinschaft Industrieller Forschungsvereinigungen) and by MWF (Ministerium für Wissenschaft und Forschung des Landes Nordrhein-Westfalen, Referat Zukunftstechnologien) is gratefully acknowledged. We are indebted to Professor Dr K. Molt of this university for his kind assistance in the establishment and interpret-

ation of the IRRAS spectroscopy. We are also grateful to Mr M. Oberst, who provided the voltammetric results.

References

[1] Europ. Pat. 55 358 (BASF, H. Naarmann et al., 12/1980).
[2] D. Bloor, R. D. Hercliffe, C. G. Galiotis and R. J. Young, in 'Electronic Properties of Polymers and Related Compounds', (edited by H. Kuzmany, M. Mehring and S. Roth), Springer, Berlin (1985) p. 179.
[3] F. Beck, in 'Encyclopedia of Material Science and Engineering', Suppl. 1 (edited by R. W. Cahn), Pergamon Press, New York (1988), pp. 140–147.
[4] F. Beck, *Electrochim. Acta* **33** (1988) 839.
[5] R. Steude, Ph.D. Thesis, Über die elektrochemische Oxidation von Pyrrolen und Pyrrolfarbstoffen. Technical University Munich (1933).
[6] A. Dall'Olio, Y. Dascola, V. Varacca and V. Bocchi, *C.R. Acad. Sci. Ser. C.* **267** (1968) 433.
[7] S. Asavapiriyanont, G. K. Chandler, G. A. Gunawardena and D. Pletcher, *J. Electroanal. Chem.* **177** (1984) 229.
[8] L. F. Warren and D. P. Anderson, *J. Electrochem. Soc.* **134** (1987) 101.
[9] A. F. Diaz, K. K. Kanazawa and G. P. Gardini, *J. Chem, Soc., Chem. Commun.* **1979**, 635.
[10] K. K. Kanazawa, A. F. Diaz, W. D. Gill, P. M. Grant, G. B. Street, G. P. Gardini and J. F. Kwak, *Synth. Met.* **1** (1979) 329.
[11] A. Diaz, *Chem. Scripta* **17** (1981) 145.
[12] A. J. Downard and D. Pletcher, *J. Electroanal. Chem.* **206** (1986) 139.
[13] F. Beck and M. Oberst, *Angew. Chem. Int. Ed.* **26** (1987) 1031.
[14] F. Beck and M. Oberst, *Makromol. Chem., Macromol. Symp.* **8** (1987) 97.
[15] E. M. Genies, G. Bidan and A. F. Diaz, *J. Electroanal. Chem.* **149** (1983) 101.
[16] F. Beck, M. Oberst and P. Braun, *DECHEMA-Monograph.* **109** (1987) 457.
[17] A. Mohammadi, O. Inganas and I. Lundström, *J. Electrochem. Soc.* **133** (1986) 947.
[18] F. Beck, P. Braun and M. Oberst, *Ber. Bunsenges. Phys. Chem.* **91** (1987) 967.
[19] L. D. Burke, J. F. Healy and O. J. Murphy, *J. Appl. Electrochem.* **13** (1983) 469.
[20] G. Wegner, W. Wernet, D. T. Glatzhofer, J. Ulanski, Ch. Kröhnke and M. Mohammadi, *Synth. Met.* **18** (1987) 1.
[21] F. Beck and M. Oberst, *Synth. Metals* **28** (1989) C43.
[22] H. Naarmann, *Makromol. Chem., Macromol. Symp.* **8** (1987) 1.
[23] M. Ogasawara, K. Funahashi, T. Demura, T. Hagiwara and K. Iwata, *Synth. Met.* **14** (1986) 61.
[24] M. Salmon, A. F. Diaz, A. J. Logan, M. Krounby and J. Bargon, *Mol. Cryst. Liqu. Cryst.* **83** (1982) 265.
[25] K. Molt, *Fresenius Z. Anal. Chem.* **319** (1984) 743.
[26] T. Shono, 'Electroorganic Chemistry as a New Tool in Organic Synthesis', Springer, Berlin (1984).
[27] Fu Ren F. Fan, B. L. Wheeler, A. J. Bard and R. N. Noufi, *J. Electrochem. Soc.* **128** (1981) 2042.
[28] T. Skotheim, L.-G. Petersson, O. Inganäs and I. Lundström, *J. Electrochem. Soc.* **129** (1982) 1737.
[29] A. J. Frank and K. Honda, *J. Electroanal. Chem.* **150** (1983) 673.
[30] R. Noufi, D. Tench and L. F. Warren, *J. Electrochem. Soc.* **127** (1980) 2310.
[31] L. Fornarini and B. Scrosati, *Electrochim. Acta* **28** (1983) 667.
[32] G. K. Chandler and D. Pletcher, *J. Appl. Electrochem.* **16** (1986) 62.
[33] H. Münstedt, H. Naarmann and G. Köhler, *Mol. Cryst. Liqu. Cryst.* **118** (1985) 129.
[34] H. Münstedt, *Polymer* **29** (1988) 296.
[35] F. Beck, Jiang Jing, M. Kolberg, H. Krohn and F. Schloten, *Z. physik. Chem.*, in press.
[36] F. Beck, P. Braun and F. Schloten, *J. Electroanal. Chem.* in press.
[37] K. M. Cheung, D. Bloor and G. C. Stevens, *Polymer* **29** (1988) 1709.